

Encapsulation and Release Behavior from Lipid Nanoparticles: Model Study with Nile Red Fluorophore

Thomas Delmas^{1,2}, Amandine Fraichard¹, Pierre-Alain Bayle³,
Isabelle Texier^{1,*}, Michel Bardet³, Jean Baudry²,
Jérôme Bibette^{2,*}, and Anne-Claude Couffin^{1,*}

¹CEA-LETI, Campus MINATEC, Département des Technologies pour la Biologie et la Santé,
17 rue des Martyrs, F-38054 Grenoble, France

²Laboratoire des Colloïdes et Matériaux divisés, ESPCI, 10 rue Vauquelin, 75231 Paris cedex 5, France

³Laboratoire de Résonances Magnétiques, SCIB, UMR-E CEA/UJF-Grenoble 1, INAC,
17 rue des Martyrs, F-38054 Grenoble, France

Lipid nanoparticles, based on nanoemulsion templates, are interesting candidates for contrast agent and active ingredient transport and delivery due to their small size, biodegradable nature and high versatility. An optimized nanosystem for drug delivery should present an important encapsulation ratio, as well as controlled release kinetics. In this context, the influence of the lipid nanoparticle core composition on the encapsulation and release behavior of the Nile Red fluorophore, used as a model molecule of intermediate lipophilicity, is explored. For that purpose, the lipid nanoparticle physical state, the encapsulated molecule localization, and the encapsulation/release behavior are studied. Careful characterization of lipid nanoparticles is performed by DSC and ¹H NMR analysis. Nile Red localization is evaluated by complementary fluorescence spectroscopy and ¹H NMR techniques. The encapsulation of Nile Red is governed and limited by its solubility in the lipids. A double localization of the fluorophore at the membrane and in the particle core is observed, resulting in a two-phase release kinetics: a quick burst release, followed by a slow prolonged release. Adding wax to the formulation increases the lipid nanoparticle internal viscosity while favoring Nile Red localization in the core, which results in slower release kinetics.

Keywords: Lipid Nanoparticles, Amorphous Physical State, Localization, Prolonged Release, Nile Red.

1. INTRODUCTION

A major challenge in nanomedicine is to engineer nanostructures and materials that can efficiently encapsulate drugs at high concentration, cross the cell membrane, and controllably release the cargo content at the target site over a prescribed period of time.^{1,2} Carriers of nanometric size are promising tools to (1) protect, (2) target and (3) improve intrinsic properties of the encapsulated molecules. Nanoencapsulation prevents the encapsulated species from direct biological interactions, thus drug or contrast agent degradation by enzymes or acid environment, and helps in reducing their potential systemic toxicity. Moreover, encapsulating active pharmaceutical

ingredients (API) can allow improving their therapeutic efficiency by controlling their biodistribution and kinetics of release.

Among a wide variety of nanocarriers, lipid-based systems present numerous advantages over other formulations. These nanocarriers are biocompatible, biodegradable and can easily be produced by versatile and up-scalable processes.^{3–5} Such nanoparticles have been employed for encapsulating a wide range of active pharmaceutical ingredients and contrast agent.⁵ Nonetheless, it is still difficult to prepare lipid nanocarriers with high encapsulation ratios of actives, while controlling their kinetics of release. The internal physical state of lipid core nanoparticles has been shown to dramatically affect the encapsulation and release properties. Nanoemulsions were the first lipid core

*Authors to whom correspondence should be addressed.

nanocarriers to be introduced decades ago, but few of these systems finally came to market due to formulation issues. Indeed, these systems suffer from low colloidal stability and sustained release is difficult to achieve due to the low viscosity of the dispersed phase.⁶ This generally leads to the rapid diffusion of the drugs out of the droplets. Solid lipid nanoparticles (SLN) have thus been proposed to overcome these limitations, thanks to their solid core. However, despite high expectations of such systems for prolonged release of hydrophobic molecules, SLN have shown limited controllability. Crystallization of the lipid phase generally leads to drug/lipid phase separation and subsequent drug expulsion, providing high burst release.^{7,8} Nanostructured lipid carriers (NLC) were introduced as a compromise. Composed of a mixture of liquid and solid lipids, the NLC core presents an imperfect crystallization which favors better encapsulation ratio thanks to lower crystallinity, while allowing control over release kinetics through the solid character of the lipid phase.⁹ Three different types of NLC have been developed: (1) the imperfect type, whose crystallinity is lowered by creating imperfections in the crystal lattices; (2) the structureless type, which is solid but amorphous; and (3) the multiple Oil/Fat/Water type, in which small droplets of liquid lipids are phase separated in the solid matrix.¹⁰

The first type has been widely reported and used to efficiently increase the encapsulation ratios while maintaining significant prolonged release.¹¹ Nonetheless, whereas the other types should theoretically allow better encapsulation/release properties, there is a discrepancy in the conclusions concerning their practical achievement. For instance, the structureless type could allow high encapsulation ratio by avoiding lipid organization, while favoring prolonged release thanks to its solid nature. However, some authors account that their lipid core is in a super cooled melt state rather than an amorphous solid.^{9,12}

In this context, our research group has proposed a new type of very stable amorphous lipid core nanoparticles (LNP).¹³ Such a nanoemulsion system can efficiently be produced by ultrasonication and possesses a long-term stability through entropic stabilization.¹⁴ In order to use these LNP as nanocarriers for drug and/or contrast agent encapsulation and delivery, their drug encapsulation and release behaviors have to be characterized. Highly hydrophobic contrast agents have already successfully been encapsulated in LNP for imaging purposes.^{15,16} In this study, the Nile Red (NR) fluorophore is used as a model molecule of intermediate lipophilicity ($\log P \sim 3-5$), such as the potent chemotherapeutic Paclitaxel, to study the influence of the lipid particle core composition on the LNP encapsulation and release behaviors. This low cost molecule, compared to active pharmaceutical ingredients, possesses microenvironment-sensitive fluorescence properties relevant for localization purposes.¹⁷⁻¹⁹ This molecule is of

interest to cost-effectively get insight into the LNP encapsulation, localization and release behaviors, before properly optimizing the system with the desired API. The present paper aims to understand how internal composition influences NR encapsulation and release profile from the lipid nanoparticles. For that purpose, we first investigate the influence of core composition on the LNP physico-chemical properties and the core physical state. We then study how it affects the encapsulation and localization of NR molecules, and finally how NR release kinetics is modified.

2. MATERIALS AND METHODS

2.1. Materials

The wax Suppocire NBTM (mixture of mono-, di- and triglycerides of alkyl chain length varying from C₁₂ to C₁₈) is a kind gift from Gattefossé (Saint-Priest, France). Myrj s40TM (polyethylene glycol 40 stearate) and Super-refined Soybean oil are kindly donated by Croda (Chocques, France). The phospholipids Lipoid s75TM (composed of >75% phosphatidylcholine) are purchased from Lipoid (Ludwigshafen, Germany). Other chemical products are purchased from Sigma Aldrich (Saint Quentin Fallavier, France).

2.2. LNP Processing

LNP are prepared by emulsion templating through ultrasonication. Both aqueous and lipid phases are separately prepared before mixing. The lipid phase contains a blend of solid (Suppocire NBTM) and liquid (Super refined Soybean oil) glycerides with phospholipids (Lipoid s75TM), while the aqueous phase is composed of a PEG surfactant (Myrj s40TM) dissolved in PBS aqueous buffer (1× Phosphate Buffer Saline: 10 mM phosphate, 154 mM NaCl, pH 7.4). Standard LNP formulations are prepared at 10% weight fraction with 1800 μ L PBS, 92 mg Myrj s40TM, 90 mg oil/wax mixture and 18 mg Lipoid s75TM. After homogenization at 45 °C, both phases are crudely mixed. Then, sonication cycles are performed at 45 °C during a 5 min period (VCX750 Ultrasonic processor, 3 mm probe, Sonics, France; sonication power 25%). Non encapsulated components are separated from LNP dispersions by gentle dialysis overnight in 1X PBS against 1,000 times their volume (MWCO: 12,000 Da, ZelluTrans). Before use, LNP dispersions are filtered through 0.22 μ m cellulosic membrane (Millipore).

In the case of LNP loaded with 0.1% w/w Nile Red, a solution of 120 μ L Nile Red 10 mM in CH₂Cl₂ is added to the oily phase and the solvent is evaporated. Then, this doped oily phase is used as aforementioned, to produce LNP encapsulating Nile Red at a local concentration of 2.3 nmol/mg dispersed phase.

Different wax/oil ratios (w/w) in the core have been used. For simplification, LNP samples are quoted NCXX where XX defines the weight fraction of wax in the LNP core (% w/w).

2.3. Characterization

2.3.1. Dynamic Light Scattering (DLS)

The particle size and zeta potential of the lipid nanoparticles are measured using a Malvern Zeta Sizer Nano instrument (NanoZS, Malvern, UK). The nanoparticle suspensions are diluted 100 folds with $0.1 \times$ PBS buffer. At least three different LNP batches are used per condition. Results are expressed in terms of mean and standard deviation of all the samples for each condition, each sample result being the mean of three independent measurements performed at 25 °C.

2.3.2. Differential Scanning Calorimetry (DSC)

DSC analysis is conducted using a TA Q200 system (TA instrument, France). Samples are weighed (2 to 5 mg for bulk material and 10 to 20 mg LNP dispersion) into standard aluminum sample pans, which are then sealed with a pinhole-pierced cover and an empty pan is used as reference. Heating curves are recorded at a scan rate of 10 K/min from 20 °C to 70 °C.

2.3.3. Viscosity of Lipid Core Mixtures at 40 °C

The rheological properties of NC0, NC50 and NC100 bulk samples are determined using an AR 2000 rheometer (TA instrument, France) with a cone and plate fixture (diameter 10 mm, angle 1°). Measurements are performed at 40 °C in order to avoid macroscopic issues of sample crystallinity. Shear rates ranging from 0.1 to 300 s⁻¹ are applied and the viscosity value is extracted from the Newtonian flow.

2.3.4. NMR Spectroscopy

¹H NMR spectra are recorded using an Avance DPX 500 spectrometer (Bruker, Wissembourg, France), operating at 500 MHz. They are processed and analyzed with the MestRe-C v3.0 software. The assignment of the ¹H and ¹³C NMR resonances of PEG-40-stearate (Myrj s40™), lecithin and triglycerides mixtures (soybean oil and supocire NC™) is achieved by standard methods with the acquisition of ¹H, ¹³C and ¹H-¹H homonuclear correlation (COSY) spectra.¹⁴ An accurate quantity of 0.1% w/w of sodium 2,2-dimethylsilapentane-5-sulphonate (DSS) (for aqueous samples) or tetramethylsilane (TMS) (for chloroform dissolved samples) is added as a 0 ppm and resolution reference. LNP spectra are recorded at temperatures ranging from 10 to 60 °C.

For localization of Nile Red molecules in the LNP structure, the 7–9 ppm spectral window is particularly explored. In order to amplify the NR signals and then selectively record them, a selective 90° eBurp proton pulse covering a spectral range of about 2000 Hz is applied.

In order to localise, at a molecular level, the NR within the LNP, homonuclear proton–proton dipolar interactions are looked for. For that purpose, ¹H NOE (Nuclear Overhauser Effect) measurements were carried out by applying a pre-saturation time of 5 s. ¹H NOE difference spectra were obtained by alternatively irradiating the peak of interest and a control point in the spectrum followed by data acquisition. For each spectrum, 2048 transients were acquired. Selective pulse was also used to favour the detection of NR compound. Data processing was performed in the frequency domain by subtracting the on-resonance and off-resonance spectra to obtain the so-called NOED-IFF (Nuclear Overhauser Effect Difference Spectroscopy) spectra. The interactions of NR with other components can be directly visualized on the resulting spectrum by the appearance of NOE signals.

2.3.5. Fluorescence Spectroscopy

NR localization study is performed using a TECAN Infinite 1000 spectrometer (TECAN, Lyon, France). First, Nile Red fluorescence spectra X_i ($\lambda_{exc} = 505$ nm) are recorded separately in the different LNP components i : pure oil (0.1% w/w dye), pure wax (0.1% w/w dye), PEG surfactant aqueous solution (with concentration > critical micelle concentration, 0.1% w/w dye), phospholipid aqueous solution (0.1% w/w dye). Each fluorescence spectrum X_i is then normalised by the fluorescence intensity integral of the NR fluorescence spectrum in the component i , to give normalized fluorescence spectrum x_i .

Fluorescence spectra Y ($\lambda_{exc} = 505$ nm) are then recorded for the different LNP samples with different wax/oil core ratios (0.1% w/w dye loading). The fluorescence spectrum of each NR-loaded LNP (as displayed in Fig. 3(a)) is then normalised by the overall fluorescence intensity under the curve, to obtain “normalized” fluorescence spectra y of Nile Red dispersed in LNP, as displayed in Figure 3(a) *insert*. In order to get qualitative information about Nile Red localization, each normalized spectrum y of LNP NCXX is then deconvoluted over the normalized NR spectra x_i obtained previously in the different LNP components, using the Excel software. For this purpose, the proper α_i coefficients allowing minimizing the difference between the experimental LNP spectrum and the fit spectrum ($y - \sum \alpha_i x_i$) with $\sum \alpha_i = 1$ are determined. α_i represents the % of Nile Red localized in the i compartment. Due to the significant spectral overlap between the fluorescence spectra of Nile Red in oil and wax on one side, which represent core compartmentation, and PEG surfactants and phospholipids on the other side, which represent shell location, qualitative NR localization is then

expressed as % of NR localized in the two main LNP structural compartments: the core (wax and oil) and the shell (PEG surfactants and phospholipids).

2.4. NR Encapsulation Efficiency

Previous to quantification of Nile Red payload in nanoparticles, the fluorophore is extracted after destruction of the nanoparticles according to the following protocol adapted from the literature.²⁰ Briefly, extraction is performed by dissolving 200 μL LNP dispersion (10% weight fraction) in tetrahydrofuran (ratio 1/3 v/v) at room temperature, followed by a selective lipid precipitation in methanol (ratio 1/2 v/v) at 4 °C. After centrifugation, the supernatant is filtered on a Minisart® 0.2 μm filter (Sartorius, Goettingen, Germany) and an aliquot of 20 μL of filtrate is analyzed by HPLC-UV method. The efficiency of this extraction protocol is >95%. Chromatographic separation is carried out on a Supelcosil C18 column (250 \times 4.6 mm, 5 μm) (Supelco, USA) using a Waters 2495 separation module with a Waters 2487 dual absorbance spectrometer (Waters, Saint-Quentin-en-Yvelines, France) at detection wavelengths of 227 nm and 552 nm. The elution is performed with an isocratic mixture of Methanol/Water (90/10 v/v) with a flow rate of 1 mL/min. With this protocol, NR retention time is 7.2 min. Quantification is achieved by comparison between the Nile Red observed peak area for $n = 3$ samples per formulation, with a calibration curve obtained under the same conditions.

The encapsulation efficiency is calculated by dividing the amount of Nile Red still encapsulated in the LNP after purification by dialysis, by the amount of Nile Red inside LNP before purification (Eq. (1)). This is performed by NR extraction and quantification over the purified samples (right after dialysis) by the previously described HPLC protocol. The maximum loading ratio is then given by the maximum payload achievable without significant loss during the purification step (encapsulation efficiency >80%).

$$\text{Encapsulation efficiency} = \frac{\text{amount of NR after dialysis}}{\text{amount of NR before dialysis}} \times 100 \quad (1)$$

2.5. In Vitro NR Release Kinetics

The release study is carried out using a dialysis protocol. In brief, after preparation, NR loaded LNP samples (300 μL of 10% dispersed phase weight fraction) are placed in 500 μL Quix Sep micro-dialysis capsules (Fisher Bioblock, Illkirch, France) and subjected to intensive dialysis in 1,000 times their volume (MWCO 12,000 Da MW, ZelluTrans). The amount of molecules still encapsulated is determined by dividing the payload of NR in LNP after different periods of time to the original payload after LNP preparation/purification, following the extraction/HPLC quantification protocol previously described.

The release rate is then given by Eq. (2). Temperature-dependent release kinetics is performed in 1 \times PBS buffer at three temperatures (4 °C, room temperature (25 °C) and 40 °C) over 8-day periods.

$$\% \text{ release} = \left(1 - \frac{\text{amount of NR after dialysis}}{\text{amount of NR before dialysis}} \right) \times 100 \quad (2)$$

3. RESULTS

3.1. LNP Formulation

The nanocarrier system described herein is based on an oil-in-water emulsion. The lipid nanoparticles (LNP) are composed of an oily core (mixture of solid and liquid lipids) which is stabilized by a surfactant shell, combination of hydrophilic (PEG surfactant) and lipophilic surfactants (phospholipids). The oily phase contains soybean oil (Super Refined Oil™), semi-synthetic wax (Suppocire NB™), or a mixture of both, in which saturated and unsaturated long-chain triglycerides (saturated C₁₂–C₁₈ for Suppocire NB™ and unsaturated C₁₆–C₁₈ for soybean oil) are present. Due to their high lipophilic character, these species have very low solubility in the continuous phase, then restraining possible destabilization of the colloidal dispersion through Ostwald ripening.¹³ Moreover, soybean oil is acknowledged for its biocompatibility, and is FDA-approved for parenteral injection. Such composition allows obtaining long term stable formulations as aqueous dispersions.^{13,14} It was previously demonstrated that adding wax to the lipid core increases LNP core viscosity.¹³ This study is focused on 50 nm-diameter particles, obtained by optimization through an experimental design.¹⁴ This formulation has been selected for its size and neutral surface charge, ensuring low polydispersity, favoring physical stability by Ostwald Ripening prevention.¹³ and passive accumulation in tumors.^{15,21}

A series of formulations with similar surfactant shell composition and constant lipid core weight are first prepared. The lipid core composition ranges from NC0 (0% wax/100% oil) to NC100 (100% wax/0% oil), while NR loading is varied from 0.01% to 0.1% w/w of the dispersed phase. Changing core composition does not affect the particle surface charge (zeta potential), while great amount of oil in lipid core tends to increase the LNP diameter (Table I). Indeed, a 10% increase in hydrodynamic diameter is observed when increasing the amount of oil in the core from pure wax to pure oil core nanoparticles. As previously detailed, such increase in LNP diameter when varying the oil/wax ratio has to be related to the differences of viscosity between the wax and oil dispersed phases during the sonication process.¹³ Meanwhile, the encapsulation of Nile Red does not significantly affect the surface charge and particle size properties. The zeta potential thus remains nearly neutral with values close to -6 mV.

Table I. LNP physicochemical properties as a function of core composition and Nile Red loading: particle hydrodynamic diameter (d) and zeta potential (ξ) (average and standard deviation over $n = 3$ samples).

NR concentration (% w/w dispersed phase)	Core composition					
	NC0		NC50		NC100	
	d (nm)	ξ (mV)	d (nm)	ξ (mV)	d (nm)	ξ (mV)
0	65.2 ± 1.3	-5.9 ± 2.1	58.9 ± 0.9	-6.0 ± 1.1	50.2 ± 2.5	-4.3 ± 0.8
0.01	64.5 ± 4.1	-7.2 ± 2.1	61.4 ± 2.9	-6.5 ± 2.3	54.6 ± 1.9	-5.2 ± 1.9
0.05	66.7 ± 4.2	-6.9 ± 2.6	62.1 ± 3.2	-5.9 ± 3.1	56.3 ± 1.8	-5.9 ± 2.4
0.1	68.4 ± 3.8	-6.5 ± 2.2	64.4 ± 3.1	-6.8 ± 2.9	55.7 ± 2.1	-6.0 ± 3.1

3.2. Influence of Core Composition on Internal Physical State

The LNP internal physical state is investigated by Differential Scanning Calorimetry (DSC) and ^1H NMR techniques.

DSC analysis allows investigating whether the lipids are crystallized. As compared to bulk lipid mix, DSC thermograms of 50 nm-diameter particles do not display any thermal event along heating from room temperature to 60 °C. It therefore indicates that lipids are under amorphous state when nanoformulated as LNP, whereas they are in a crystalline state as a bulk. This was observed to be true whatever the LNP internal composition from NC0 to NC100 (0% wax to 100% wax) over 8-month storage at both 4 °C and room temperature.

The LNP internal viscosity was monitored by NMR spectroscopy by following the evolution of LNP ^1H NMR spectra as function of core composition and temperature. Indeed, peak resolution is related to molecular mobility: when increasing the viscosity of a sample, peak resolution is seen to decrease in liquid-state ^1H NMR through peak broadening. In extreme limit for a completely solid matrix, no signal is expected to appear in spectra recorded under liquid-state NMR conditions. As previously described, in the LNP ^1H NMR spectrum, it is possible to assign specific signals representative of particle locations.¹⁴ Two signals (labeled by square and triangle symbols) are located at 1.3 ppm and 3.7 ppm, respectively attributed to the methyl protons of alkyl chains and the methylene protons of PEG surfactant (Fig. 1(a)). Whatever core composition, the width related to PEG chain peaks does not change while temperature decreases from 35 °C to 10 °C, as depicted by peak width ratio close to 0.9–1.0 in Figure 1. These chains belonging to the external membrane and being exposed to water are not significantly affected by changes in the lipid core internal composition. On the contrary, when looking at a peak specific to the internal lipids (1.3 ppm), significant differences can be observed. Indeed, whereas the peak width ratio is close to 0.95, and thus the peak resolution only slightly decreases when going from 35 °C to 10 °C in the case of pure oil core (NC0), loss of resolution and peak broadening are more significant with a core composed of 50% oil/50% wax (NC50) and even more

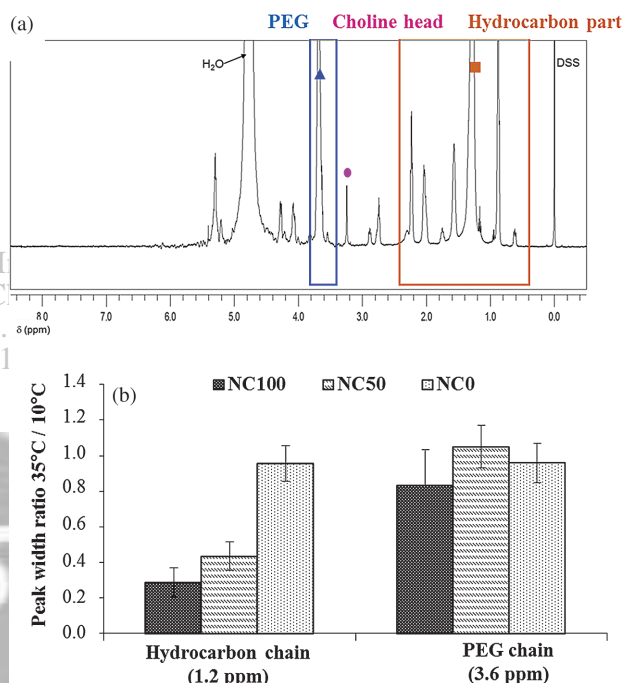


Fig. 1. Particle internal viscosity assessed by ^1H NMR. (a) ^1H -NMR spectrum of LNP NC75 at room temperature. (b) Peak width ratio at two different temperatures (10 °C and 35 °C), as a function of core composition (NC0, NC50 and NC100).

when looking at a pure wax core LNP (NC100), these two compositions displaying peak width ratios of respectively 0.45 and almost 0.25 (Fig. 1(b)). These differences in peak resolution account for significant differences in viscosities, depending on core composition and temperature. The more wax in the core and the colder, the more viscous.

3.3. Nile Red Encapsulation Efficiency

The influence of core composition on the maximum NR payload is investigated by formulating LNP of different wax/oil core ratio with increasing amounts of Nile Red. The encapsulation efficiency is determined following NR extraction from nanoparticles by quantification using the HPLC protocol described in the Materials and Methods section (Fig. 2). The maximum accessible loading ratio is given by the maximum payload achievable without significant loss during the purification process. The limit of

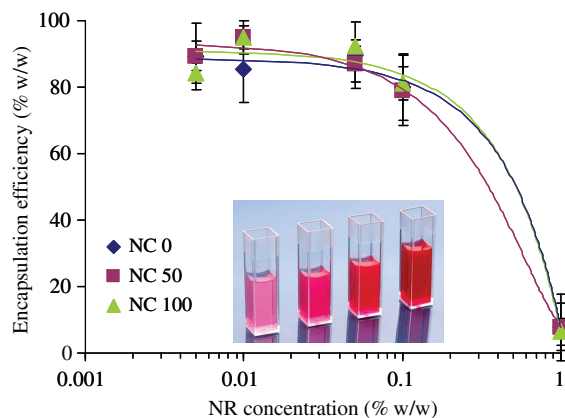


Fig. 2. Nile Red encapsulation: determination of the maximum payload (mean and standard deviation over $n = 3$ samples per condition) for different core compositions (NC0: diamond symbol, NC50: square symbol, NC100: triangle symbol). A picture of LNP encapsulating Nile Red at increasing concentrations is given at a glance.

significant loss is fixed at 20% since the LNP processing efficiency is close to 80–85% due to the low volumes used, which leads to some material loss on the glass vials. All core compositions behave similarly, giving a maximum payload of around 0.1% w/w (Fig. 2). Modulating the core composition by varying the wax/oil core ratio therefore does not allow modifying the NR loading ratio.

3.4. Nile Red Localization

Nile Red localization is investigated by fluorescence and ^1H NMR studies. As Nile Red fluorescence is known to be very sensitive to its microenvironment,^{17,22} this feature is used to evaluate the dye localization once encapsulated in LNP of different core compositions. The NR fluorescence spectra while dispersed at 0.1% w/w in pure oil, pure wax, or in PEG or phospholipid aqueous solutions are recorded (Fig. 3(a) *insert*). As already described in the literature, fluorescence intensity and peak maximum shift are observed.^{17,18} Apolar environment (oil and wax) lead to emission maxima of ≈ 580 – 610 nm, whereas more polar environment (phospholipids and PEG surfactants) lead to an emission maximum of around ≈ 630 – 640 nm. Fluorescence spectra recorded for the different NR loaded LNP compositions are reported in Figure 3(a), highlighting significant differences depending on particle core composition. It is also noticed that these fluorescence profiles have a very large bandwidth in comparison to the emission bands observed for NR in the presence of each ingredient taken separately (Fig. 3(a)). Therefore, it appears that NR loaded LNP emission results from the different components. Each LNP fluorescence spectrum is therefore deconvoluted over the four different components to achieve a qualitative analysis of NR localization (Materials and Methods section). Nevertheless, the significant overlapping of NR fluorescence within LNP membrane components (phospholipids and PEG surfactant) and LNP core

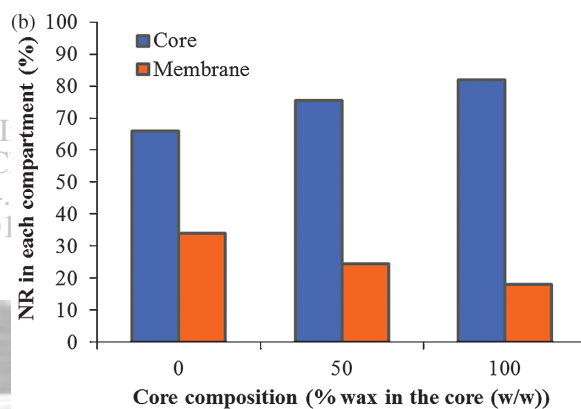
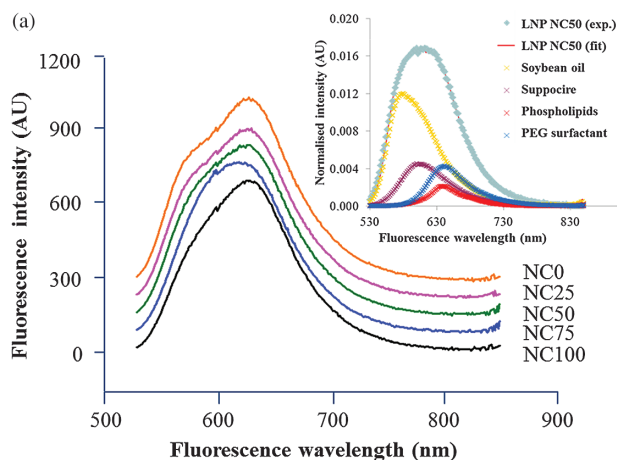


Fig. 3. Nile Red localization assessed by fluorescence analysis. (a) Fluorescence spectra of Nile Red-loaded LNP with different core compositions; *insert*: deconvolution of the fluorescence spectrum of Nile Red-loaded LNP NC50, using Nile red fluorescence spectra in the different components of LNP (soybean oil, Suppocire NBTM, phospholipids, Myrj 53TM). (b) Nile Red localization as a function of LNP core composition.

components (wax and oil) lead us to consider two-partition localization for NR molecules (core and shell compartments). This analysis reveals that Nile Red is located both in the membrane and in the lipid core with various percentages (Fig. 3(c)). Interestingly, the relative proportion of Nile Red at the particle shell or into the core depends on the lipid core composition. Indeed, the more wax in the core, the more NR is located into the core.

To gain further insight into this NR double localization, NR loaded LNP of NC75 core composition (75% wax/25% oil) are studied by classic ^1H NMR spectroscopy and NOEDIFF (Nuclear Overhauser Effect Difference Spectroscopy) experiment. First, a temperature study is performed, recording the evolution of peak resolution and width associated to NR molecules as a function of temperature. As can be seen in Figure 4(a), the resolution of Nile Red peaks dramatically decreases when cooling the system from 35 °C to 10 °C (focus in the 7.0 to 9.0 ppm range, for which only Nile Red peaks are observed). This decrease in peak resolution is related to a decrease in molecular

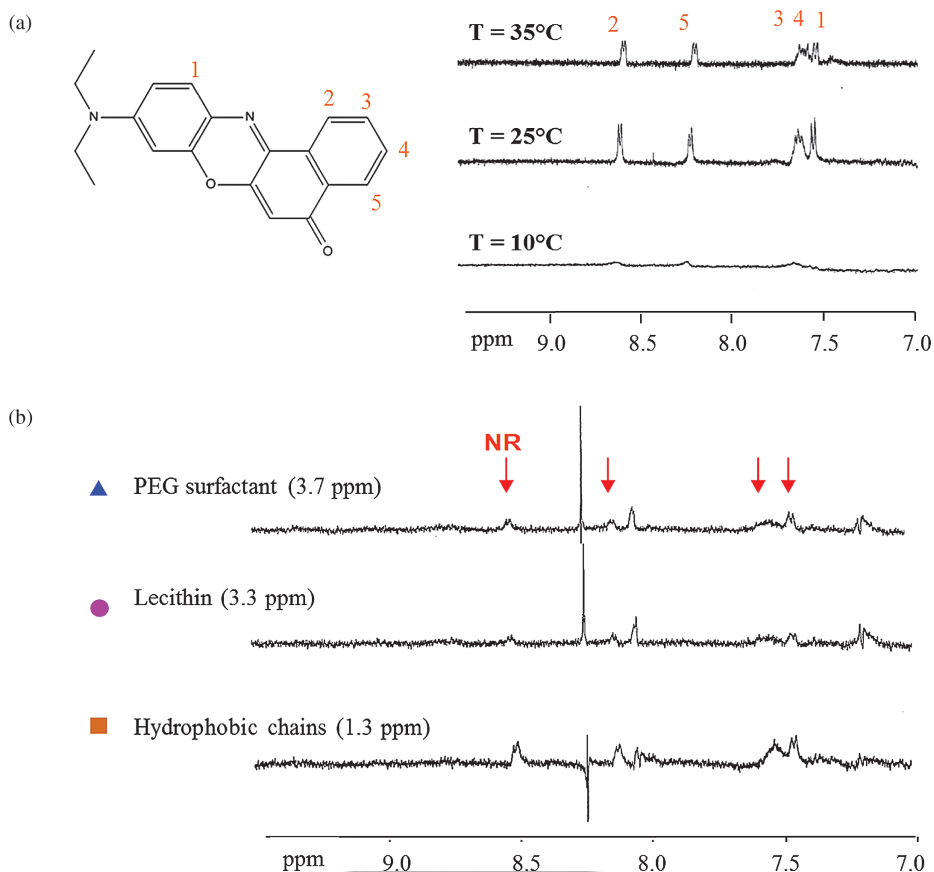


Fig. 4. Nile Red localization assessed by NMR study. (a) Nile Red chemical structure and selective pulse: effect of the temperature. (b) NOEDIFF spectra at 25 °C by irradiation of respectively 3.7, 3.3 and 1.3 ppm signals (Nile Red specific peaks are marked by an arrow). Formulation used: NC75 encapsulating 0.1% w/w NR.

mobility, due to a microenvironment viscosity increase, as explained above for core components. Nonetheless, even at 10 °C, it is still possible to observe peaks, even though they are dramatically broaden. This qualitatively supports the fact that most NR molecules are localized in the particle core, but also suggests that a part of them remains located at the surface, when considering a NC75 core composition. To finally conclude about NR localization, complementary quantitative NOEDIFF experiments are performed. The principle is to use NOE transfer to localize NR molecules in the LNP structure, by evaluating the efficiency of magnetization transfer between LNP components and NR molecules. The characteristic NMR peaks associated to PEG chains (3.7 ppm), choline heads of the lecithin (3.3 ppm) and hydrocarbon part (1.3 ppm) of the core components are thus excited individually and the effect on Nile Red signals is assessed (Fig. 4(b)). For similar excitation conditions, larger signals are obtained when exciting core components (hydrophobic chains) compared to PEG chains or lecithin. Yet, here again, some signals are still observed with membrane components (lecithin and PEG). These NOEDIFF results are consistent with a double localization, already suggested by fluorescence spectroscopy. These findings confirm that most of NR

molecules localizes in the core while a small amount also localizes at the membrane of LNP.

3.5. Nile Red *In Vitro* Release

The influence of core composition and temperature on Nile Red release kinetics is then investigated. For that purpose, LNP formulations with 3 different wax/oil ratios (NC0, NC50, NC100) at the maximum payload (0.1% w/w NR) are prepared and purified, before undergoing *in vitro* release under dialysis at different temperatures: 4 °C, 25 °C and 40 °C. The results are displayed in Figure 5. Each release curve presents two noticeable parts: (1) a quick burst release, occurring during the first 5 hours; and (2) a slow prolonged release for times >5 hours. When considering the burst release, no significant temperature effect is observed and 20–30% of the encapsulated molecules escape from LNP during the first 5 hours of the experiments. Temperature has a more pronounced influence on the prolonged release. Indeed, whereas no significant prolonged release is observed over 150 hours at 4 °C and 25 °C, 70–80% NR molecules are released at 40 °C after the same time. More interestingly, whereas no influence of core composition is observed at 4 °C and

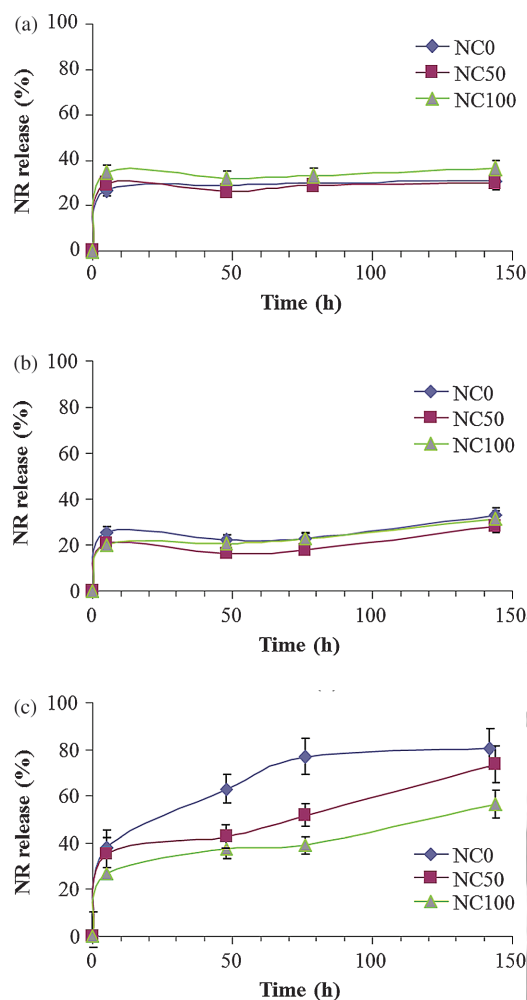


Fig. 5. Nile Red *in vitro* release at different temperatures: (a) 4 °C, (b) 25 °C and (c) 40 °C. LNP of 3 different core compositions loaded with 0.1% NR w/w are compared: NC0 (diamond symbol), NC50 (square symbol) and NC100 (triangle symbol).

25 °C on the burst and prolonged release, significant differences occur at 40 °C. Increasing the amount of wax in the core thus leads to a reduced burst release (up to 40% for NC0, 35% for NC50 and less than 25% for NC100) (Fig. 5(c)). Similarly, increasing the amount of wax in the core leads to slower prolonged release kinetics. For NC0 LNP, NR release levels off at 80% of total NR molecules after 75 hours. In parallel, such level of release is reached after 150 hours for NC50 LNP, and is still not achieved after 150 hours for NC100 LNP samples.

4. DISCUSSION

4.1. Influence of Dye Solubility and Localization on Encapsulation

LNP core composition does not significantly change their NR loading capabilities, and different core compositions lead to similar maximum loading of about 0.1% w/w. This

has to be related to the NR solubility in the melted macroscopic mixtures of lipid compounds (Table II). Indeed, NR is slightly more soluble in wax containing mixtures after 3 weeks storage at room temperature. Nonetheless, NR crystallizes in all lipid mixtures when at concentrations higher than 0.1% w/w. Both liquid and solid lipids are triglycerides with similar chemical entities. Soybean oil is composed of fatty acids with C_{16} – C_{18} alkyl chain length, while Suppocire NB™ is a more complex mixture of mono-, di- and triglycerides with various lengths of alkyl chain ranging from C_{12} to C_{18} with a hydroxyl value of 20–30%. Therefore, the presence of partial di- and monoglycerides and the variation in chain length could improve the NR solubility in the presence of the wax. However, all tested lipid mixtures exhibit a solubility limit close to 0.1% w/w in lipid bulks. As NR has a double localization once nanoformulated (in the core and in the membrane), this slight variation of core solubility (lipid solubility) could be compensated by a membrane re-localization, making all LNP samples display a similar 0.1% w/w maximum loading capacity. This low loading can be explained by the low lipophilicity of the NR molecule ($\log P = 3.5$) and is emphasized by the huge amount of hydrophilic surfactants corresponding to almost 50% w/w of the dispersed phase. This loading ratio is well below the classical 10% API content, as encountered in well-established pharmaceutical formulations, which should be sufficient to allow the required therapeutic dose of API to be administrated. In comparison, loading ratios up to 6–10% w/w in LNP have been successfully achieved for molecules with higher lipophilic character such as the DiD fluorophore.¹⁶ or photosensitizers used in photodynamic therapy. Although chemical modifications of the desired API may be performed in order to increase its lipophilicity by alkyl chains grafting, the LNP system offers a promising suitability as high lipophilicity API delivery systems.

Yet, whereas not significantly impacting the maximum loading achievable, changing core composition notably affects NR localization, as demonstrated by fluorescence and NMR studies (Figs. 3 and 4). Adding wax to the particle core promotes localization of NR molecules inside the lipid core instead of at the membrane compartment. This

Table II. Nile Red solubility in bulk lipid mixtures just after preparation (t_0) and after 3-week storage at 25 °C: soluble (sol.), insoluble (×) and appearance of a few crystals (\approx).

Bulk lipid mixtures	NR concentration (% w/w dispersed phase)					
	0.05		0.1		0.25	
	t_0	$t_0 + 3$ weeks	t_0	$t_0 + 3$ weeks	t_0	$t_0 + 3$ weeks
NC0	Sol.	Sol.	Sol.	×	×	×
NC50	Sol.	Sol.	Sol.	\approx	×	×
NC100	Sol.	Sol.	Sol.	Sol.	×	×

feature is consistent with the preferential solubility of NR dye in wax compared to soybean oil.

4.2. Release Profiles

As evidenced in Figure 5, the NR release profile from LNP presents a two-step process: (1) a burst release and (2) a prolonged release. It has first to be noted that LNP size remains nearly constant along the release experiments, therefore suggesting that NR release does not rely on particle destabilization. The burst release frees around 20–30% of total NR molecules during the first 5 hours of experiments. At 4 ° and 25 °C, the amount of released molecules is not significantly affected by core composition. However, at 40 °C, increasing the amount of wax in the core leads to decreased burst release. Interestingly, the amount of NR molecules released during the burst phase increases with the amount of NR localized at the membrane as quantified by the fluorescence measurements (Fig. 6(a)). These NR molecules, belonging to the shell in contact with the continuous aqueous phase, could easily be released due to osmotic pressure exerted on the PEG surfactant by high dilution and intensive dialysis in micro dialysis capsules. This occurrence can lead to surfactant desorption

and could account for the observed burst release. To further support this hypothesis, a complementary NR release experiment is performed, lowering the osmotic pressure on the surfactants by saturating the release medium with surfactants (with a surfactant PEG concentration > critical micelle concentration). As shown in Figure 6(b), burst release occurs during the first 15 minutes and is significantly reduced under saturated medium conditions. After 2 hours, both releases become similar, probably due to the solubilization of NR in the presence of PEG surfactants micelles.

Meanwhile, the Nile Red prolonged release is notably affected by temperature and core composition (Figs. 5, 7). Indeed, whereas no prolonged release is observed at 4 °C and 25 °C, a significant release is obtained at 40 °C and the kinetics of release is dramatically slowed down when adding wax to the LNP core (Fig. 7(a)). As no convection process can exist on such nano-compartment, Nile Red release should be related to the diffusion of the NR molecules through the LNP structure, in particular through the lipid matrix, as already described for other lipid nanocarriers.^{23,24} Since the nanoscale does not allow us to assess the micro-viscosity of the particle lipid core, we performed viscosity measurements on the lipid bulks at 40 °C (temperature for which all lipid blends are under

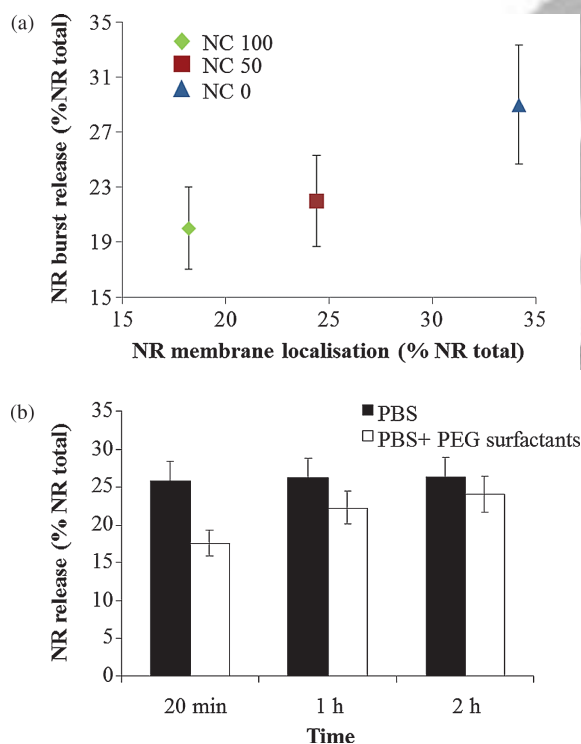


Fig. 6. Nile Red burst release. (a) Correlation between Nile Red membrane localization (assessed by fluorescence spectroscopy) and Nile Red burst release for 3 different core compositions (NC0, NC50, NC100) at 25 °C. (b) Nile Red release from NC100 LNP loaded with 0.1% w/w fluorophore: release at 40 °C in PBS versus release at 40 °C in PBS saturated with PEG surfactants (Mirj s40™, above their critical micelle concentration).

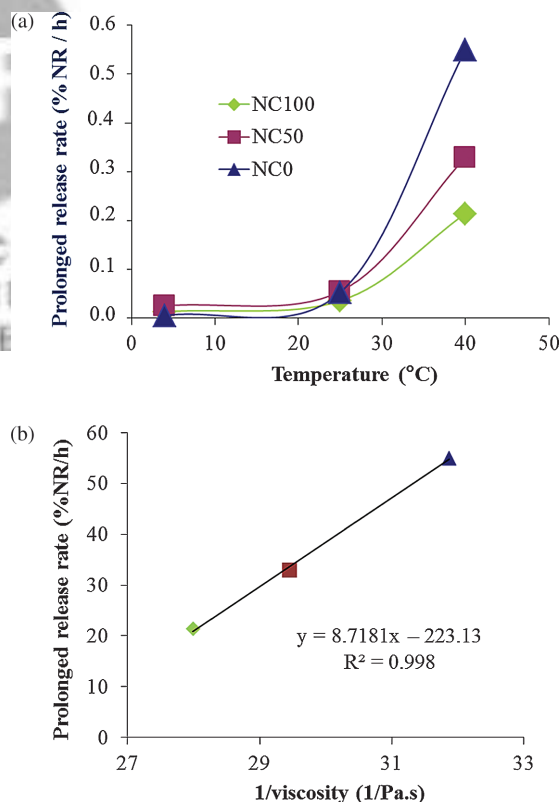


Fig. 7. Nile Red prolonged release. (a) Effect of temperature and composition on Nile Red prolonged release. (b) Correlation between the viscosity of the bulk lipid mixtures (NC0, NC50 and NC100) and prolonged LNP release kinetics at 40 °C.

liquid form). As shown in Figures 7(b), at 40 °C, the prolonged release kinetics scales as the inverse of the lipid mixture viscosity, as expected for a diffusion-driven process according to the Einstein-Stokes law. It is indicative that the prolonged release kinetics mainly depends on the intrinsic micro-viscosity of the LNP core. Diffusion of molecules is a temperature-activated process.²⁵ From this study, it can be stated that it is possible to modify the release kinetics by varying the core composition and the temperature release conditions, which affect the microviscosity and the associated local diffusion coefficient of the encapsulated molecules.

5. CONCLUSION

The relationship between the core composition of lipid nanoparticles, their internal physical state, the localization of encapsulated species and their encapsulation/release properties was here studied using Nile Red as a model of intermediate lipophilic molecule. We demonstrated the amorphous character of LNP and further underlined that changing the particle core composition allows its internal physical state to be tuned from very fluid to highly viscous. Changing the LNP core composition has been shown to change the Nile Red localization and dramatically affect NR release. Whatever release condition, a burst release which may rely on desorption of PEG surfactants was observed in the first 5 hours. Under storage conditions (4 °C and 22 °C), we expect no significant leakage as long as no surfactant desorption can occur. Under physiological conditions, the release kinetics is mainly driven by the internal physical state of LNP nanoparticles. Increasing the amount of wax in the core is shown to significantly slow the Nile Red release kinetics. Attempts will be made in further investigations to reinforce the LNP shell by modifying membrane composition and making it more rigid, and therefore limiting burst release. The micro-viscosity of the LNP core, related to lipid composition, could help controlling the release kinetics. This fundamental understanding of the physicochemical basis directing the kinetics of release should now allow the fine tuning of such behavior for further applications of the LNP nanocarrier as a drug delivery system.

Abbreviations

API: Active Pharmaceutical Ingredient; DLS: Dynamic Light Scattering; DSC: Differential Scanning Calorimetry; LNP: Lipid NanoParticles; NOEDIFF: Nuclear Overhauser Effect Difference Spectroscopy; NR: Nile Red; PBS: Phosphate Buffer Saline.

Acknowledgments: We acknowledge the Molinspiration Property Calculation Service (www.molinspiration.com) for logP calculation. The authors thank Catherine Picart and Thomas Boudou for help during the fluorescence measurements, and Rachel Auzely and Eric Bayma for rheology support. This work was supported by the Commissariat à l'Énergie Atomique et aux Énergies Alternatives (CEA), and the French National Research Agency (ANR) through Carnot funding.

References and Notes

1. V. P. Torchilin, *Adv. Drug Deliv. Rev.* **58**, 1532 (2006).
2. L. Zhang, F. X. Gu, J. M. Chan, A. Z. Wang, R. S. Langer, and O. C. Farokhzad, *Clin. Pharmacol. Ther.* **83**, 761 (2008).
3. M. D. Joshi and R. H. Müller, *Eur. J. Pharm. Biopharm.* **71**, 161 (2009).
4. W. Mehnert and K. Mäder, *Adv. Drug Deliv. Rev.* **47**, 165 (2001).
5. R. H. Müller, K. Mäder, and S. H. Gohla, *Eur. J. Pharm. Biopharm.* **50**, 161 (2000).
6. B. Mangenheim, M. Y. Lvy, and S. Benita, *Int. J. Pharm.* **94**, 115 (1993).
7. H. Bunjes, M. H. J. Koch, and K. Westesen, *Langmuir* **16**, 5234 (2000).
8. C. Freitas and R. H. Müller, *Eur. J. Pharm. Biopharm.* **47**, 125 (1999).
9. H. Bunjes, K. Westesen, and M. J. H. Koch, *Int. J. Pharm.* **129** (1996).
10. R. H. Müller, M. Radtke, and S. A. Wissing, *Int. J. Pharm.* **242**, 121 (2002).
11. E. B. Souto and R. H. Müller, *Handbook of Experimental Pharmacology*, edited by M. Schäfer-Korting, Heidelberg (2010), pp. 115–141.
12. K. Westesen and H. Bunjes, *Int. J. Pharm.* **115**, 129 (1995).
13. T. Delmas, H. Piraux, A. C. Couffin, I. Texier, F. Vinet, P. Poulin, M. E. Cates, and J. Bibette, *Langmuir* **27**, 1683 (2011).
14. T. Delmas, A. C. Couffin, P. A. Bayle, F. de Crécy, E. Neumann, F. Vinet, M. Bardet, J. Bibette, and I. Texier, *J. Colloid Interf. Sci.* **360**, 471 (2011).
15. I. Texier, M. Goutayer, A. Da Silva, L. Guyon, N. Djaker, V. Jossierand, E. Neumann, J. Bibette, and J. Vinet, *J. Biomed. Opt.* **14**, 054005 (2009).
16. J. Gravier, F. Navarro, T. Delmas, F. Mittler, A. C. Couffin, F. Vinet, and I. Texier, *J. Biomed. Opt.* **16**, 096013 (2011).
17. P. Greenspan and S. D. Fowler, *J. Lipid Res.* **26**, 781 (1985).
18. A. Y. Jee, S. Park, and M. Lee, *Chem. Phys. Lett.* **477**, 112 (2009).
19. C. Lin, J. Zhao, and R. Jiang, *Chem. Phys. Lett.* **464**, 77 (2008).
20. A. Lamprecht and J. P. Benoît, *J. Chromat. B* **787**, 415 (2003).
21. M. Goutayer, S. Dufort, V. Jossierand, A. Royère, E. Heinrich, F. Vinet, J. Bibette, J. L. Coll, and I. Texier, *Eur. J. Pharm. Biopharm.* **75**, 137 (2010).
22. V. Teeranachaideekul, P. Boonme, E. B. Souto, R. H. Müller, and V. B. Junyaprasert, *J. Control. Release* **128**, 134 (2008).
23. V. Teeranachaideekul, R. H. Müller, and V. B. Junyaprasert, *Int. J. Pharm.* **340**, 198 (2007).
24. J. J. Wang, K. S. Liu, K. C. Sung, C. Y. Tsai, and J. Y. Fang, *Eur. J. Pharm. Sci.* **38**, 138 (2009).
25. J. Guery, J. Baudry, D. A. Weitz, P. Chaikin, and J. Bibette, *J. Phys. Rev. E* **79**, 060402(R) (2009).

Received: 15 February 2012. Accepted: 6 March 2012.